PNAS RESEARCH ARTICLE | EVOLUTION OPEN ACCESS

Distinct latitudinal patterns of molecular rates across vertebrates

Tianlong Cai[a,b,c], Zhixin Wen[d], Zhongguan Jiang[e], and Ying Zhen[a,b,c,1]

Affiliations are included on p. 7.

Edited by Dolph Schluter, University of British Columbia, Vancouver, BC, Canada; received November 12, 2024; accepted April 10, 2025

The latitudinal diversity gradient (LDG) is the most notable global biodiversity pattern, but its underlying mechanisms remain unresolved. The evolutionary speed hypothesis (ESH) posits that molecular rates play a crucial role in shaping the LDG, suggesting that higher temperatures accelerate molecular rates, thereby facilitating rapid speciation and accumulation of biodiversity in the tropics. However, whether ESH can explain the LDG across diverse taxonomic groups remains debated, and systematic examinations of its two key predictions using consistent datasets and methodologies across vertebrates are lacking. Here, we tested ESH using molecular rates from mitochondrial (5,424 species) and nuclear (1,512 species) genomes across major vertebrate groups, including fishes, amphibians, reptiles, mammals, and birds. Our findings revealed distinct latitudinal patterns in the absolute synonymous substitution rate (dS), which were influenced by thermoregulatory strategies. Specifically, the dS increases with ambient temperature and decreases with latitude in ectotherms but shows no correlation in most endotherms. These distinct patterns are likely attributed to different key predictors of dS between thermogroups, with temperature playing a major role only in ectotherms. For mitochondrial genes, absolute nonsynonymous substitution rates (dN) increase with temperature, likely driven by mutation rates in ectotherms and purifying selection in endotherms. However, neither mitochondrial dS nor dN correlates with diversification rates across vertebrates, contradicting the second prediction of ESH. For nuclear rates, the ESH was supported in reptiles and amphibians but not in mammals, birds, or fishes. In conclusion, our results provide limited support for ESH in vertebrates, underscoring the intricate processes that shape the LDG.

molecular rate | latitudinal diversity gradient | evolutionary speed hypothesis | temperature | thermoregulation

Significance

Increasing species richness toward the equator has been hypothesized to result from elevated temperatures, which increase molecular rates and consequently facilitate rapid speciation. We tested this hypothesis using 5,424 mitochondrial and 1,512 nuclear genomes of vertebrates to explore latitudinal patterns in molecular rates and their relationships with species diversification. Our findings reveal that neutral molecular rates increase with temperature in ectotherms but not in endotherms, reflecting distinct key predictors between thermogroups. Nonneutral mitochondrial rates increase with temperature across vertebrates, but mitochondrial molecular rates do not correlate with species diversification. Nuclear molecular rates support this hypothesis in reptiles and amphibians but not in mammals, birds, or fishes. Our findings suggest that factors beyond molecular rates drive global biodiversity patterns across vertebrates.

The latitudinal diversity gradient (LDG) is the most prominent biodiversity pattern observed globally across most organisms (1). The mechanisms underlying LDG remain debated, with many hypotheses attributing it to faster speciation rates in the tropics (2, 3). One evolutionary explanation for higher tropical speciation rates is the kinetic effects of temperature on molecular rates (4–6), which may subsequently influence the accumulation of genetic incompatibility or the level of genetic variation that natural selection could act upon (7, 8). The evolutionary speed hypothesis (ESH) thus posits that elevated tropical temperatures lead to faster molecular rates through higher mutation rates, shorter generation times, and/or stronger selection, which facilitate faster rates of speciation and the accumulation of diversity (9). The ESH makes two predictions: Molecular rates depend on ambient temperature, and diversification rates (DRs) depend on molecular rates (10, 11).

The temperature dependence of the molecular rates can be explained by metabolic theory (6). Basal metabolic rates (BMR) are determined by body mass and body temperature (12). Mutations are tightly linked to various processes influenced by metabolism, including oxygen-free radical damage, replication errors, and DNA repair (5, 6, 13). As a result, mutation rate and neutral substitution rate are proportional to the mass-specific BMR and thus are positively correlated with body temperature and negatively correlated with body mass (5, 6). However, the effects of ambient temperature on molecular rates may differ for species with different thermoregulatory strategies. In ectotherms, molecular rates are expected to increase with ambient temperature and decrease with latitude, as their body temperature and mass-specific BMR vary passively with ambient temperature (5). In contrast, endotherms maintain stable body temperatures through metabolic heat production, with low ambient temperatures potentially driving increased mass-specific BMR to sustain thermoregulation (14–16). However, the effects of ambient temperature on molecular rates of endotherms are less clear and have yet to be explored.

Extensive efforts have been made to test ESH; however, no consensus has been reached from empirical data in various taxonomic groups (Dataset S1). This is partially due to variations in methodologies and genetic markers used among studies. Moreover,

Author contributions: T.C. and Y.Z. designed research; T.C. and Y.Z. performed research; T.C., Z.W., and Z.J. analyzed data; and T.C. and Y.Z. wrote the paper.

The authors declare no competing interest.

This article is a PNAS Direct Submission.

[1]To whom correspondence may be addressed. Email: zhenying@westlake.edu.cn.

This article contains supporting information online at https://www.pnas.org/lookup/suppl/doi:10.1073/pnas.2423386122/-/DCSupplemental.

Published May 8, 2025.

comprehensive tests of ESH require the evaluation of both predictions (10, 11), but few studies have done so (10). Whether ESH could explain the LDG across diverse taxonomic groups remains debated (17, 18). To address the above challenges, we estimated and analyzed the absolute species-specific molecular rates across fishes, amphibians, reptiles, birds, and mammals. We demonstrated distinct latitudinal and temperature-dependent patterns of neutral molecular rates across vertebrates. We found a lack of correlation between mitochondrial molecular rates and DRs and limited support for ESH from only nuclear molecular rates in reptiles and amphibians.

Results

Distinct Latitudinal Patterns in Mitochondrial dS between Endotherms and Ectotherms. We compiled a comprehensive dataset of publicly available vertebrate mitochondrial genomes from NCBI and estimated species-specific absolute synonymous (dS) and nonsynonymous (dN) substitution rates per year of 12 mitochondrial genes using a phylogeny-based approach (19, 20) (*SI Appendix*, Fig. S1). This method weights relative molecular rates by divergence times, which are calibrated with 169 fossils (Dataset S2). Because synonymous mutations are generally considered neutral, the neutral theory of molecular evolution predicts their substitution rate as $dS = 2N_e\mu \times (1/2N_e) = \mu$, where N_e is the effective population size, μ is the mutation rate (21, 22). Thus, dS is equivalent to the mutation rate, whereas dN is affected by the mutation rate, genetic drift, and selection (21, 22). The estimated molecular rates varied significantly across vertebrates (Fig. 1), spanning three orders of magnitude (Dataset S3). On average, fishes, amphibians, and reptiles have lower molecular rates than mammals and birds do (*SI Appendix*, Fig. S2), which is likely attributed to the higher mass-specific BMRs in endotherms than in ectotherms (13, 23).

At the species level, using the absolute latitude of distribution centroids and average ambient temperatures across full distributions, we observed distinct latitudinal patterns (t = −200.71, df = 3,756, P < 0.001) and temperature dependences (t = 280.10, df = 3,640, P < 0.001) of dS between endotherms and ectotherms (Fig. 2 and *SI Appendix*, Figs. S3–S5). Specifically, after accounting for phylogenetic signals (*SI Appendix*, Fig. S6) using Bayesian phylogenetic generalized linear mixed models (PGLMMs), dS increased with temperature in ectotherms (slope [95% CI]: 0.16 [0.11, 0.20], P_{MCMC} < 0.001), particularly in fishes (0.15 [0.10, 0.21], P_{MCMC} < 0.001), amphibians (0.15 [0.03, 0.27], P_{MCMC} = 0.019), and reptiles (0.26 [0.14, 0.37], P_{MCMC} < 0.001). In contrast, no associations were detected between dS and temperature (P_{MCMC} = 0.20) or latitude (P_{MCMC} = 0.25) in endotherms, except for birds, whose dS decreased with temperature (–0.06 [–0.10, –0.01], P_{MCMC} = 0.024; Fig. 2*A* and Dataset S4). Additionally, dN tends to decrease with latitude and increase with temperature across all groups (ectotherms: 0.07 [0.02, 0.12], P_{MCMC} = 0.001; endotherms: 0.07 [0.04, 0.11], P_{MCMC} < 0.001; mammals: 0.08 [0.02, 0.14], P_{MCMC} = 0.008; and birds: 0.09 [0.02, 0.15], P_{MCMC} = 0.007) (Fig. 2*B*). dN/dS tends to decrease with temperature in ectotherms (–0.07 [–0.11, –0.01], P_{MCMC} = 0.01) but to increase with temperature in endotherms (0.09 [0.05, 0.12], P_{MCMC} < 0.001] (Fig. 2*C*). These results are robust to different evolutionary models, random effects, or the exclusion of species with relative molecular rates ≥ 0.4 substitutions/site (Datasets S5–S8). Consistent patterns were also observed at the assemblage level (Fig. 2 *D*–*I*, *SI Appendix*, Figs. S7–S9, and Dataset S9), where molecular rates were averaged across species within unique ecoregions (24), and spatial simultaneous autoregressive (SAR) models were used to assess the effects of temperature or latitude.

Differences in the Main Predictors of Mitochondrial dS between Endotherms and Ectotherms. To explore the underlying mechanisms shaping the observed latitudinal patterns in molecular rates, we used PGLMMs to examine the extent to which ambient temperature influences molecular rates after accounting for other highly correlated life-history traits, including body mass, longevity, age at maturity, and fecundity (*SI Appendix*, Fig. S10). dS, a proxy for the mutation rate, was also incorporated as a fixed variable to examine its impact on dN (21, 22). The incorporation of phylogeny into the models significantly increased their predictive power, especially for dS and dN/dS (Fig. 2*J* and Dataset S10). The best models explained 94.1% (dS), 65.2% (dN), and 82.7% (dN/dS) of the total variance, with phylogeny contributing 79.4%, 19.7%, and 75.3%, respectively (Fig. 2*K*), indicating that phylogenetic conservatism is stronger in dS than in dN. The best-fit models demonstrated significant interactions between specific fixed variables and thermogroups, suggesting varied impacts of fixed variables on dS, dN, and dN/dS among thermogroups (Dataset S11).

Notably, the main predictor of dS differs between thermogroups (Fig. 2*L* and Dataset S12), which likely explains the distinct latitudinal patterns of dS observed between thermogroups. In ectotherms, ambient temperature is the strongest predictor of dS (0.14 [0.09, 0.19], P_{MCMC} < 0.001), whereas in endotherms, body mass is the major predictor of dS (–0.35 [–0.45, –0.26], P_{MCMC} < 0.001), with temperature showing no significant effect (P_{MCMC} = 0.16). For dN, dS is the strongest predictor (ectotherms: 0.31 [0.27, 0.35], P_{MCMC} < 0.001; endotherms: 0.18 [0.13, 0.22], P_{MCMC} < 0.001; Fig. 2*M*), and temperature has a positive effect on dN in endotherms (0.08 [0.04, 0.11], P_{MCMC} < 0.001). dN/dS was negatively correlated with temperature in ectotherms (–0.07 [–0.12, –0.02], P_{MCMC} = 0.011) but positively correlated with temperature in endotherms (0.08 [0.05, 0.12], P_{MCMC} < 0.001) (Fig. 2*N* and *SI Appendix*, Fig. S11). These results are also robust to evolutionary models, random effects, or the exclusion of species with incomplete traits or relative molecular rates ≥ 0.4 substitutions/site (Datasets S13–S16).

No Correlation between DRs and Mitochondrial Molecular Rates. The ESH predicts that DRs increase with increasing molecular rates. To test this hypothesis, we used a sister-pairs method to examine the correlation between DRs and molecular rates. Specifically, we selected 215 nonoverlapping sister lineages at the family level (Dataset S17), each sharing a unique common ancestor exclusive to other pairs in the tree. We conducted regressions using the differences in clade sizes and molecular rates between two lineages of species pairs. Our results indicated that there was a positive association between differences in clade size and differences in dS only in birds (P = 0.007) (Table 1 and *SI Appendix*, Fig. S12) but not in other vertebrate groups (P = 0.052–0.966). Moreover, no statistically significant associations between differences in clade size and differences in dN or dN/dS were found in any group (P = 0.179–0.835).

Testing ESH Using Nuclear Molecular Rates. Molecular rates of nuclear and mitochondrial genomes can vary dramatically (25), and it is debated which genome contributes more to species diversification. Here, we curated available genome-wide orthologous protein-coding genes across 1,512 vertebrate species spanning 0.25 to 3.24 Mb and estimated nuclear molecular rates. Like mitochondrial dS, nuclear dS increased with temperature in ectotherms (0.14 [0.10, 0.18], P_{MCMC} < 0.001), including fishes (0.21 [0.05, 0.34], P_{MCMC} = 0.003), amphibians (0.27 [0.13, 0.40], P_{MCMC} < 0.001), and reptiles (0.23 [0.14, 0.34],

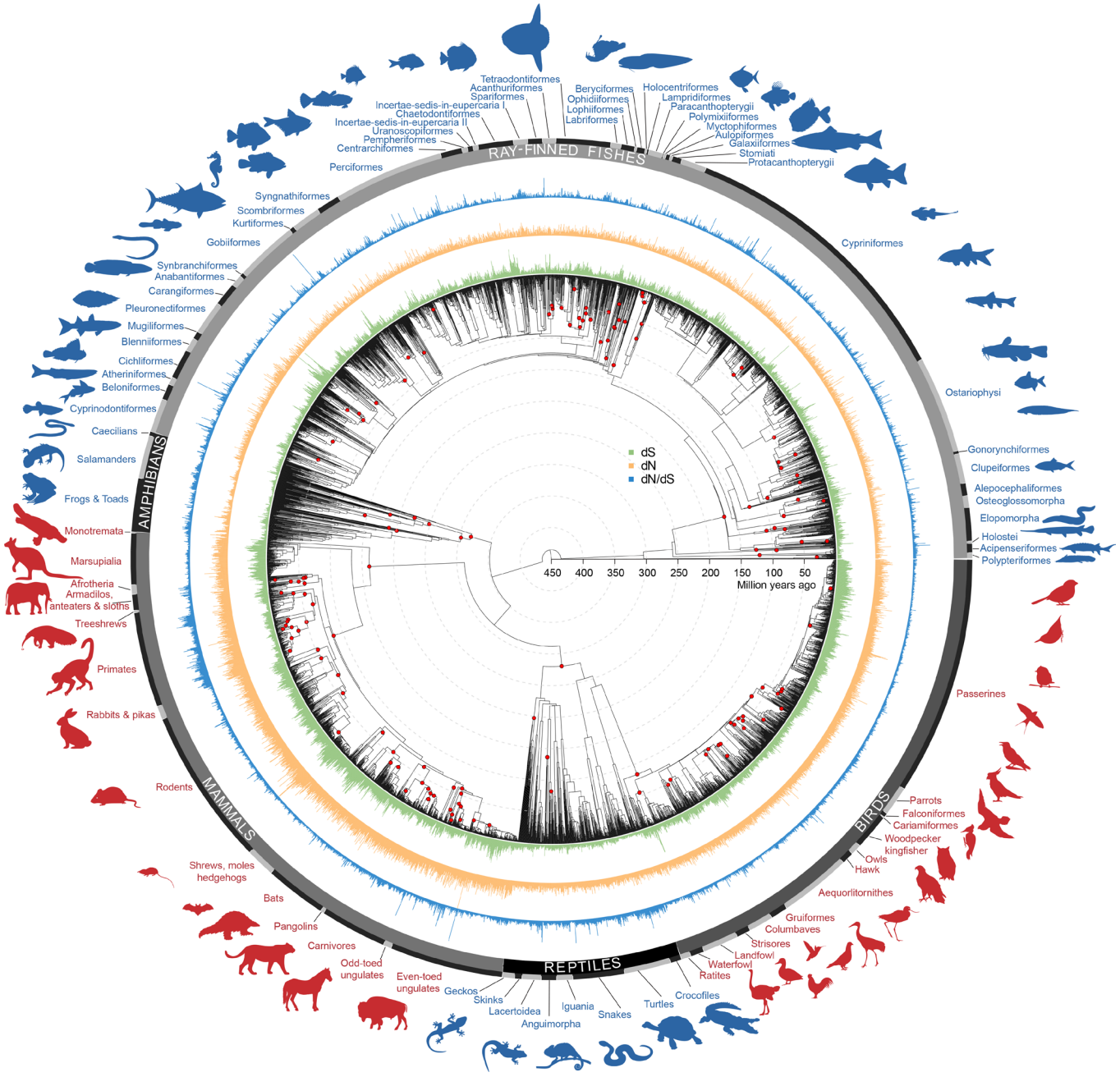

Fig. 1. Variation in mitochondrial molecular rates across vertebrate species (n = 5,424). Variations in species-specific absolute molecular rates (dS and dN) and dN/dS values are shown in the green, orange, and blue bar plots, respectively. The red points on the internal nodes of the tree are the fossil calibrations used for estimating divergence times. Silhouettes of representative species were modified from Google images. Red indicates endotherms, whereas blue indicates ectotherms.

P_{MCMC} < 0.001) (Fig. 3*A*, *SI Appendix*, Fig. S13, and Datasets S18–S21). In contrast to ectotherms (t = 197.93, df = 3,978, P < 0.001), no such correlation was found in endotherms (P_{MCMC} = 0.98). Unlike mitochondrial dN, nuclear dN generally does not correlate with temperature, except in reptiles (0.21 [0.11, 0.31], P_{MCMC} < 0.001; Fig. 3*B*). dN/dS decreased with temperature in ectotherms (−0.26 [−0.31, −0.21], P_{MCMC} < 0.001) but increased with temperature in birds (0.11 [0.02, 0.20], P_{MCMC} = 0.015; Fig. 3*C*). At the assemblage level, similar trends were observed, except that dN decreased with temperature in endotherms (Fig. 3 *D*–*I* and Dataset S22).

Unlike mitochondrial genes, body mass is the main predictor of dS in both ectotherms (−0.20 [−0.28, −0.13], P_{MCMC} < 0.001) and endotherms (−0.24 [−0.39, −0.08], P_{MCMC} = 0.001) (Fig. 3*J*, *SI Appendix*, Fig. S14, and Datasets S23–S25). Similar to mitochondrial dS, temperature positively influenced dS in ectotherms (0.12 [0.08, 0.17], P_{MCMC} < 0.001) but not in endotherms (P_{MCMC} = 0.846), which is consistent with latitudinal patterns of dS. dS is the strongest predictor of dN (Fig. 3*K*). Temperature is negatively correlated with dN (−0.14 [−0.18, −0.11], P_{MCMC} < 0.001) and dN/dS (-0.25 [−0.31, −0.20], P_{MCMC} < 0.001) in ectotherms but not in endotherms, suggesting stronger purifying selection for ectotherms at higher temperatures.

We found positive associations between differences in dS or dN and differences in clade sizes in sister pairs of amphibians, reptiles, and birds (Table 1 and *SI Appendix*, Fig. S15). Combined with the above temperature dependence of nuclear molecular rates, we found that ESH is supported only in amphibians and reptiles.

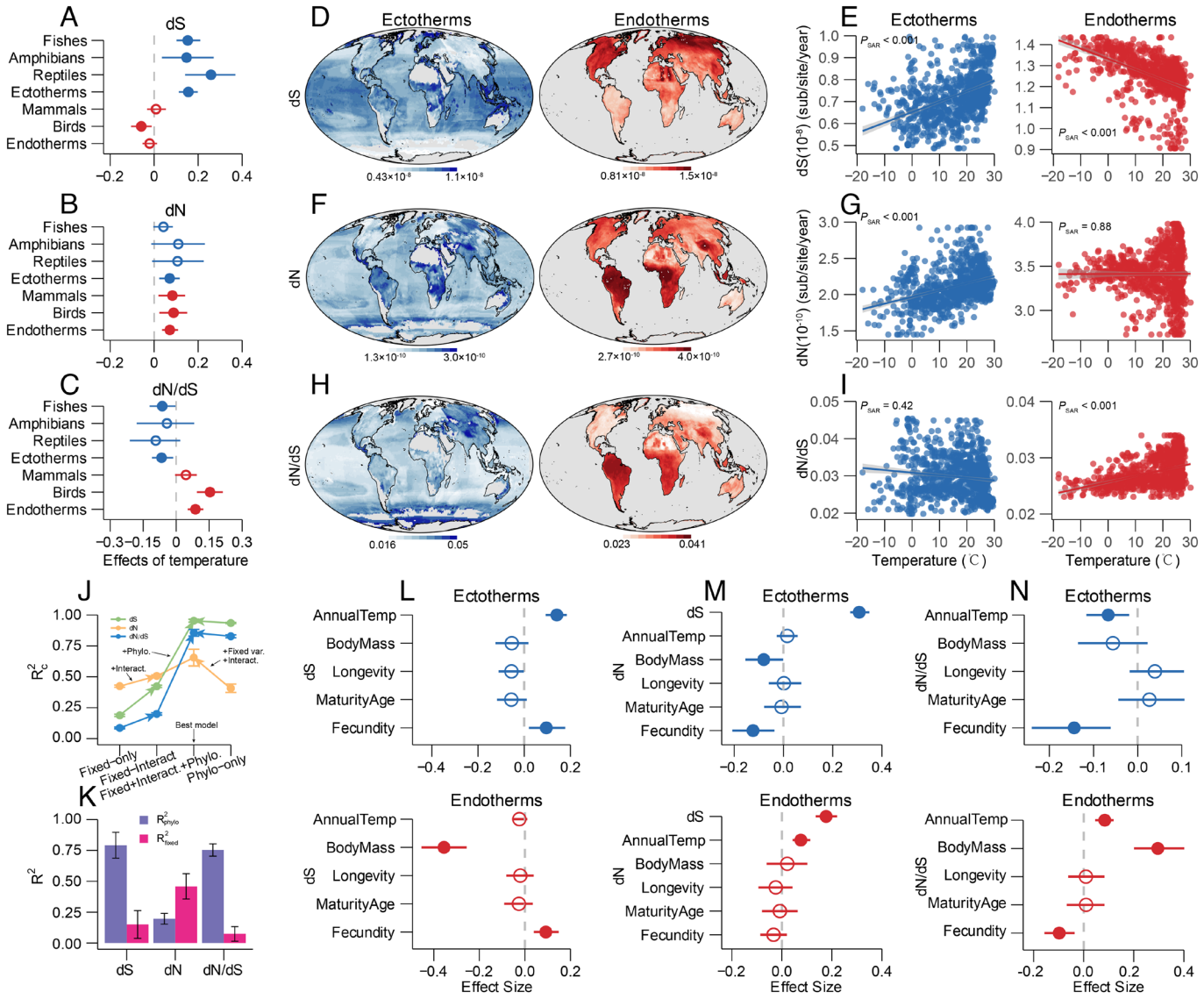

Fig. 2. Temperature dependence and latitudinal patterns of mitochondrial molecular rates. (*A–C*) Slopes of dS, dN, and dN/dS at the species level with temperature, with 95% CIs. Filled points indicate statistical significance ($P_{MCMC} < 0.05$). (*D–I*) Global distributions of molecular rates and dN/dS (1° grid-based geometric means, excluding cells with < 5 species) and their temperature relationships across ecoregions, with statistical significance tested by SAR models. (*J*) Incorporation of phylogenetic relatedness and interactions improves model fitting (conditional R^2, R_c^2) for molecular rates. (*K*) Relative contributions of fixed effects and phylogeny to molecular rate variation in the best-fit model. (*L–N*) Effect sizes and 95% CIs for predictors of molecular rates and dN/dS in endotherms and ectotherms.

Discussion

To determine whether LDG could be explained by ESH, we tested its two predictions using species-specific molecular rates from mitochondrial and nuclear genomes of vertebrates. We found that both mitochondrial and nuclear dS exhibit distinct latitudinal and temperature-dependent patterns contingent on vertebrate class and thermoregulatory strategy, which are consistent with metabolic theory but contradict the first prediction of ESH in endotherms. For mitochondrial genes, while dN generally increases with temperature across vertebrates, molecular rates do not correlate with species DRs in most vertebrate classes, contradicting the second prediction of ESH. For nuclear genes, ESH is supported in reptiles and amphibians but not in mammals, birds, or fishes. These results highlight fundamental differences between ectotherms and endotherms, as well as between mitochondrial and nuclear genomes, challenging the generality of ESH as an explanation for LDG across vertebrates.

The ESH predicts that higher temperatures in the tropics result in elevated molecular rates (9). This is supported by the observed positive correlations between dS and temperature in ectotherms, both before and after accounting for other highly correlated life-history traits, whereas no such relationship was observed in endotherms. The distinct latitudinal and temperature-dependent patterns in dS could be attributed to the different effects of ambient temperature on mass-specific BMR and mutation rates between ectotherms and endotherms. In ectotherms, body temperature varies passively with ambient temperature (5). An increase in ambient temperature leads to elevated body temperature and mass-specific BMR (6, 12), the latter of which is tightly coupled with oxygen-free radical damage and replication errors, ultimately resulting in increased mutation rates (6, 13, 26). This is supported by previous studies showing the contribution of environmental temperatures to variation in neutral substitution rates in Australian Eugongylinae skinks (27) and that higher temperatures can increase both metabolic rates and mutation rates in laboratory cultures of *Escherichia*

Table 1. Relationships between dS, dN, dN/dS, and net DRs in vertebrates

		Mitochondrial genes				Nuclear genes			
Relationship	Group	β	SE	t	P	β	SE	t	P
DR~dS	Fishes	0	0.02	0.04	0.966	0.01	0.06	0.16	0.876
	Amphibians	−0.06	0.04	−1.57	0.167	0.09	0.02	4.23	**0.001**
	Reptiles	−0.08	0.04	−2.13	0.052	0.08	0.03	2.67	**0.016**
	Mammals	0	0.04	0.09	0.927	0.03	0.03	0.98	0.332
	Birds	0.04	0.01	2.80	**0.007**	0.05	0.02	2.62	**0.011**
DR~dN	Fishes	−0.01	0.03	−0.39	0.699	0.02	0.05	0.45	0.655
	Amphibians	−0.03	0.04	−0.93	0.389	0.07	0.02	4.50	**0**
	Reptiles	−0.02	0.03	−0.53	0.602	0.07	0.03	2.16	**0.045**
	Mammals	0.03	0.03	0.76	0.451	0.01	0.03	0.30	0.768
	Birds	0.02	0.02	0.86	0.392	0.04	0.02	2.24	**0.029**
DR~dN/dS	Fishes	−0.01	0.02	−0.47	0.637	0.01	0.02	0.59	0.561
	Amphibians	0.01	0.04	0.22	0.835	−0.02	0.01	−1.67	0.113
	Reptiles	0.06	0.04	1.42	0.179	−0.01	0.02	−0.74	0.468
	Mammals	0.03	0.04	0.63	0.536	−0.02	0.01	−2.75	**0.009**
	Birds	−0.02	0.02	−1.25	0.217	−0.01	0.00	−1.94	0.058

Statistically significant differences are indicated by ordinary least squares regressions through the origin. Parameters with $P < 0.05$ are shown in bold.

coli (28). However, the impact of ambient temperature on mutation rates in endotherms is negligible because of the decoupling of body temperature and BMR from ambient temperature. Although ESH also suggests that higher ambient temperature might accelerate molecular rates by reducing generation times (9), our results show that generation time, proxied by age at maturity, has no significant effect on the molecular rates (Figs. 2*L* and 3*J*). These findings underscore fundamental differences in the mechanisms shaping mutation rates of ectotherms and endotherms in response to environmental temperature.

The decreased mitochondrial dS with increasing temperature in birds might be partially attributed to migratory birds, which have higher mass-specific BMRs due to the demands of long-distance movement (14) and predominantly breed at high latitudes (29). Our results confirm that migratory birds have significantly higher dS than resident species after accounting for body mass and

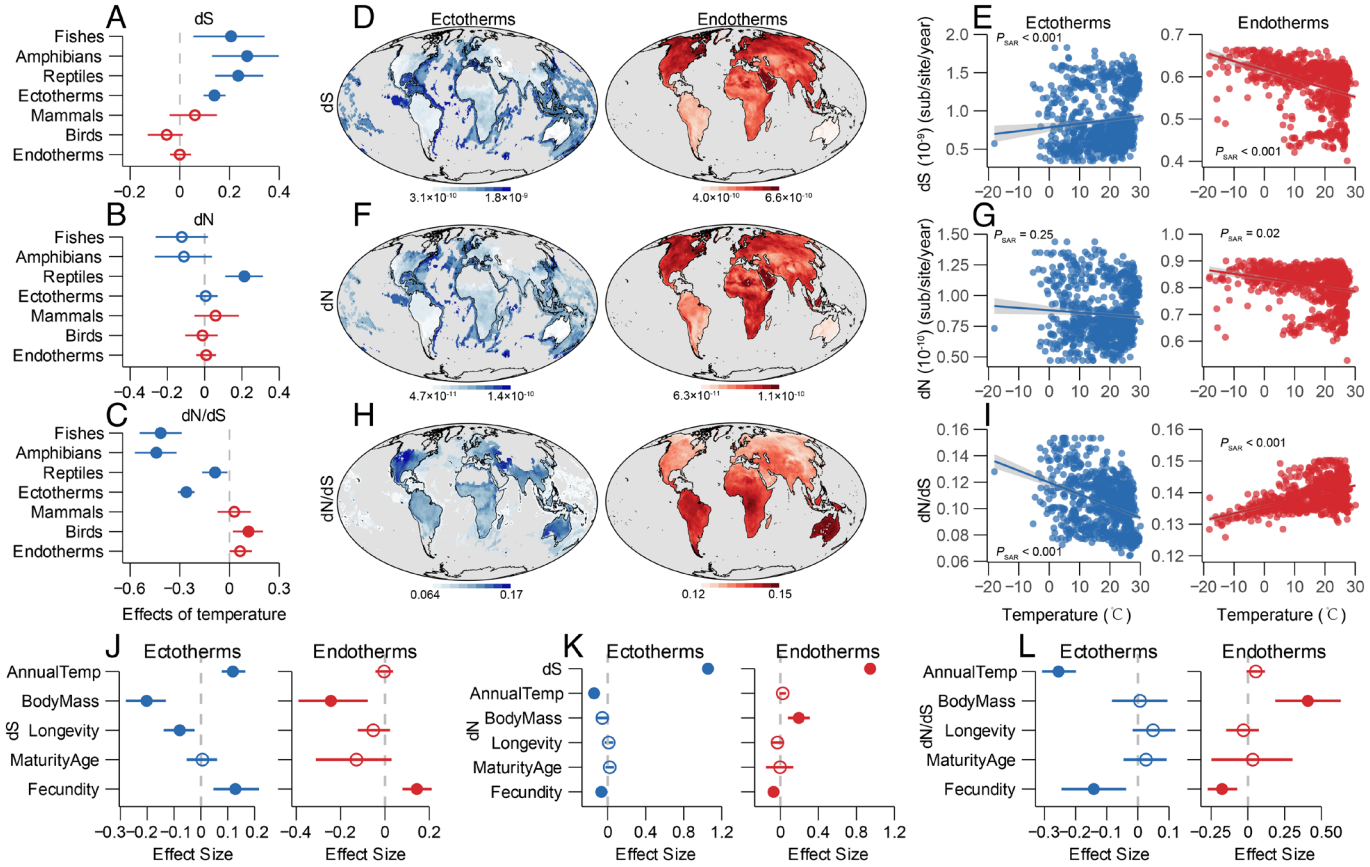

Fig. 3. Temperature dependence and latitudinal patterns of nuclear molecular rates. (*A–C*) Slopes of dS, dN, and dN/dS with temperature at the species level across groups, with 95% CIs. Filled points indicate statistical significance ($P_{MCMC} < 0.05$). (*D–I*) Global distribution of molecular rates and dN/dS values at the assemblage level and and their temperature relationships across ecoregions, with statistical significance tested by SAR models. (*J–L*) Effect sizes and 95% CIs for the predictors of dS, dN, and dN/dS in endotherms and ectotherms.

phylogenetic signals (*SI Appendix*, Fig. S16 *A* and *B*). However, even when migrants are excluded, dS remains negatively correlated with temperature (Datasets S4 and S6–S8), suggesting that other factors play a role. Cold adaptation in endotherms often involves increased BMR and heat production (14–16). This physiological strategy is prevalent in birds, whereas mammals often rely on behavioral adaptations, such as burrowing and hibernation, to conserve energy in cold environments (30, 31). Consistent with this hypothesis, we found that the mass-specific BMR in birds increased at cold temperatures, even after accounting for body mass, body temperature, migratory status, and phylogenetic relatedness (*SI Appendix*, Fig. S16*C*). These results suggest that the increased dS at colder high latitudes in birds may be attributed to both migratory behavior and physiological adaptations to cold climates.

Mitochondrial dN tends to be positively correlated with temperature in vertebrates, whereas this trend is largely absent in nuclear genes, except in reptiles. Because synonymous mutations are considered neutral, according to the neutral theory of molecular evolution, their substitution rate (dS) equals the mutation rate, whereas dN is affected by the mutation rate, genetic drift, and selection (21, 22). The genome-wide dN/dS ratio, typically below one, reflects relative strength of purifying selection and drift and is related to N_e (21, 32). Given that dN = dS × dN/dS, understanding the relationship between dN and temperature requires consideration of the contributions of both dS and dN/dS. As a result, we found that the positive correlation between mitochondrial dN and temperature arises from distinct mechanisms in endotherms and ectotherms. In ectotherms, mitochondrial dS is positively correlated with temperature, and since dS (a proxy for mutation rate) is a major predictor of dN (Fig. 2*M*), this correlation is likely driven by mutation rates. In contrast, this is unlikely to be the case in endotherms because dS does not show positive temperature dependency, and in birds, dS and dN even show opposite relationships with temperature. Instead, mitochondrial dN/dS is positively correlated with temperature (Fig. 2*N*), indicating that the observed positive correlation between dN and temperature probably is driven by dN/dS. This is likely explained by stronger purifying selection of mitochondrial genes in colder environments for endotherms to maintain highly efficient thermoregulation (14–16). Additionally, N_e could also influence dN through its effect on dN/dS and/or mutation rates. In species with large N_e, selection removes weakly deleterious mutations more efficiently, leading to reduced dN/dS (33). Moreover, the drift-barrier hypothesis suggests that mutation rates are under selection, resulting in a negative correlation between mutation rate and N_e (34, 35). However, N_e could not explain the positive correlations between dN and temperature. If tropical species generally have larger N_e than temperate species do due to Pleistocene glaciation (36), their dN/dS and mutation rates both should be lower, leading to lower dN in the tropics and an expected negative correlation with temperature, which contradicts our observations. Overall, the positive correlation between mitochondrial dN and temperature results from the combined effects of mutation, selection, and drift, with mutation rate as the primary driver in ectotherms and purifying selection as the key driver in endotherms, reflecting divergent evolutionary responses to environmental temperature between thermogroups.

For mitochondrial molecular rates, a positive correlation was found only in birds between DRs and dS but not dN, and there was no correlation between DRs and either dS or dN in any other class. For nuclear molecular rates, we observed positive associations between DRs and both nuclear dN and dS in amphibians, reptiles, and birds, which is consistent with the findings of previous studies (10, 37–39), but not in mammals or fishes. These positive associations are consistent with the second prediction of ESH and suggest that higher mutation rates, particularly nuclear rather than mitochondrial mutation rates, may promote speciation in certain groups of vertebrates. Higher mutation rates might promote speciation by accelerating the rate of reproductive isolation through increasing hybrid incompatibility or generating more beneficial variants for natural selection to act upon (7, 8). However, speciation is also influenced by ecological opportunities, adaptive divergence, and demographic history (7, 17, 40), and their relative contributions likely vary across groups. Additionally, a recent study suggested that the rate of reproductive isolation alone is not a strong predictor of diversification (41), potentially explaining why the positive association between the diversification and molecular rate is limited to specific groups.

Several limitations should be considered. First, species' geographic ranges are dynamic over evolutionary time, and our results may be influenced by historical range shifts, particularly in temperate species due to Pleistocene glaciation (36). Second, whole-genome sequences for ectotherms, particularly amphibians and reptiles, remain limited. We used genome-wide ultraconserved elements (UCEs) to estimate nuclear molecular rates in ectotherms, so this dataset is less uniform than the mitochondrial dataset across vertebrates. Future availability of whole-genome sequences will enable more robust analyses. Third, the scarcity of fossils for small vertebrates (e.g., frogs, passerines, and lizards) may hinder the accurate estimation of divergence times and absolute molecular rates. Finally, we acknowledge that substitution saturation may not be fully eliminated, however, we show that our results are robust when multiple strategies were implemented to minimize its impact.

In summary, based on the correlation patterns between temperature molecular rates, as well as between molecular rates and DRs, our results suggest that mitochondrial molecular rates do not support either predictions of ESH across vertebrate classes. In contrast, nuclear molecular rates support both predictions only in reptiles and amphibians but not in mammals, birds, or fishes. These findings challenge the generality of ESH in explaining LDG across vertebrates and suggest that alternative hypotheses need to be explored to better comprehend the general pattern of global biodiversity. More broadly, our results highlight the fundamental differences between drivers of evolutionary rates of mitochondrial and nuclear genomes, as well as between thermogroups in their responses to environmental temperature.

Materials and Methods

Estimating Rates of Molecular Evolution. We obtained mitochondrial genome data from NCBI and nuclear genome or UCE data from published sources (details in the *SI Appendix*). After quality control and filtering, 5,624 mitochondrial sequences (10 to 10.6 kb) from 1,113 birds, 1,354 mammals, 393 reptiles, 225 amphibians, and 2,539 fishes, as well as 1,702 nuclear sequences (0.25 to 3.24 Mb) from 468 birds, 421 mammals, 279 reptiles, 272 amphibians, and 262 fishes were used for subsequent analysis. Absolute molecular rates were estimated using a phylogeny-based approach following Nabholz et al. (19, 20) (*SI Appendix*, Fig. S1). First, divergence times were inferred from amino acid alignments with fossil-based calibrations. Second, the relative substitution rates of nucleotide sequences were independently estimated in small subclades, controlling for the effect of lineage-specific substitution saturation under the three models. Finally, species-specific absolute molecular rates were calculated by calibrating relative substitution rates using divergence times for terminal branches. This approach maximizes the utilization of reliable, albeit limited and ancient, fossil calibrations in vertebrates and enables rate estimation for rapidly evolving mitochondrial DNA (19).

We inferred the maximum likelihood (ML) topologies from nucleotide sequences using RAxML 8.2.4 (42), which constrains deep nodes at the order or family level with established backbone trees of birds (43, 44), mammals (45), amphibians (46), reptiles (47, 48), and fishes (24) (*SI Appendix*, Fig. S17).

Divergence times were calibrated using the penalized likelihood method in treePL (49), which incorporates 169 validated fossils to constrain internal nodes and estimates from the literature for crown age (Dataset S2). To minimize saturation effects, divergence times were estimated from ML trees on the basis of amino acid sequences. We reconstructed amino acid trees with 100 bootstrap replicates, constrained by the best ML nucleotide topology. The optimal parameters ("opt," "optad," and "optcvad") were selected from five "prime" analyses based on the lowest scores. The smoothing parameters were optimized using cross-validation with random subsampling (49), which was repeated five times to ensure stability. The lowest smoothing value, allowing greater rate heterogeneity, was used for the final dating analyses (47). To reduce variance in molecular rate estimation in recently diverged lineages (50), one species was randomly excluded from each sister pair with a divergence time < 1 My.

Substitution saturation is lineage-specific and has a greater impact on long branches than on short ones (51). To mitigate this effect, we divided the taxonomic groups into smaller subclades (587 subclades for mitochondrial data and 241 subclades for nuclear data; 2 to 30 species, mean = 9 species) with shorter evolutionary times, and then estimated dN and dS in each subclade independently (*SI Appendix*, Fig. S1). For subclades with only two species, an outgroup from the closest related subclade was randomly selected to improve substitution rate reliability, although outgroup rates were excluded from subsequent analyses. For each subclade, we checked the saturation plot using three models (K81, GG95, and TN93) and ensured that model-corrected pairwise genetic distance remained below 0.4 substitutions/site for each model (19). This threshold was chosen because our saturation plots showed that substitution saturation was relatively minor when the model-corrected pairwise genetic distance remained below this value. Additionally, species-specific absolute molecular rates were estimated using only the terminal branches (*SI Appendix*, Fig. S1*E*), which were even shorter, making them less susceptible to substitution saturation. Together, our approach has taken into account of lineage-specific substitution saturation and minimizes its impact on our rate estimations.

Relative substitution rates for all branches within each monophyletic group were estimated using the free-ratio model in the CODEML module of PAML 4.9 (52). We compared two substitution models: F3×4 (CodonFreq = 2) and F61 (CodonFreq = 3). We did not assume a molecular clock (clock = 0) or equal amino acid distances (aaDist = 0) and allowed different ω ratios for each branch (free-ratio model) and one ω ratio to vary among sites (model = 1, Nssites = 0 and fix_omega = 0), with the transition/transversion rate (κ) estimated from the data (fix_kappa = 0). Each analysis was performed three times to ensure robustness. The molecular rates estimated by the F3×4 and F61 models were highly consistent (Spearman's correlation, ρ = 0.96 to 1.00; *SI Appendix*, Fig. S18), suggesting that different codon models had minimal impact on the results. We only used the F3×4 model for subsequent analyses. Absolute species-specific dN and dS rates per year (Datasets S27 and S28) were calculated by weighting relative rates with divergence times.

Assessing Latitudinal Variation in Molecular Rates at the Species Level. Phylogenetic signals were computed using Pagel's λ in the phytools (53). To assess the relationships between molecular rates and ambient temperature or absolute midpoint latitudes, we employed Bayesian phylogenetic models that accounted for phylogenetic signals under both the Brownian model and the best-fit evolutionary model (Datasets S5 and S19). The models included a phylogenetic covariance matrix and random effects to control for the dependence of monophyletic lineages and habitat type. Before modeling, the molecular rates were log-transformed, and all variables were standardized (mean = 0 and SD = 1) to facilitate effect size comparisons. PGLMMs were run in MCMCglmm v2.34 (54) with 60,000 MCMC iterations, a burn-in of 10,000, and thinning every 25 steps, yielding 2,000 posterior samples.

Assessing Latitudinal Variation in Molecular Rates at the Assemblage Level. Latitudinal patterns of molecular rates were assessed at the assemblage level by mapping average molecular rates of vertebrates within 1° grid cells globally. Average values were calculated using the geometric means and medians of all species in each specific group per grid, excluding cells with < 5 species. To account for spatial autocorrelation and reduce computational demands, we followed Rabosky et al. (24) by analyzing the relationships between molecular rates and temperature/absolute latitude in 827 terrestrial and 232 marine ecoregions. SAR models were applied using the absolute latitude of each ecoregion's centroid or average temperature as the predictor and accounting for spatial autocorrelation between ecoregions under the best spatial distance model (24). SAR models were implemented using the function "lagsarlm()" in the R package spatialreg v1.2-6 (55). All variables were standardized (mean = 0 and SD = 1) before modeling.

Exploring Main Predictors of Molecular Rates. To assess the relative effects of fixed and random variables on molecular rates, we calculated the marginal R^2 (R_m^2) for fixed effects and conditional R^2 (R_c^2) for full models (fixed + random effects) in the PGLMMs (56). The R^2 of the phylogeny (R_{phy}^2) was calculated as R_c^2 minus R_m^2 of the PGLMMs, which included only phylogenetic relatedness as a random effect. We quantified the variation explained by fixed effects, random effects, and their combination in seven models (Dataset S10) to examine the relative effects of phylogenetic relatedness, fixed variables, and their interactions with different groups on molecular rates. Model comparisons were based on the Deviation Information Criterion. Before modeling, molecular rates, body mass, and life-history traits were log-transformed to improve normality and linearity, followed by standardization (mean = 0, SD = 1). MCMC chains were run for 60,000 iterations with a burn-in of 10,000 and thinning of 25, yielding 2,000 posterior samples. Chain convergence was confirmed through visual inspection, and autocorrelation was assessed using the "autocorr" function, with a target threshold of 0.1. Multicollinearity was evaluated via variance inflation factors.

Examining Relationships between DRs and Molecular Rates. We used a sister-pair method to examine the correlation between DRs and molecular rates on the basis of differences in molecular rates and clade sizes between sister lineages (50, 57). Each lineage was labeled at the family level according to the established phylogeny of birds (43, 44, 58), mammals (59), amphibians (60), reptiles (48, 61), and fishes (24). Three criteria were employed to select phylogenetically independent sister lineages (39): i) Representatives of chosen families formed a single clade in the phylogenetic tree; ii) each sister lineage formed an exclusive monophyletic group distinct from all other families in the tree; and iii) pairwise nucleotide distances between any two species were < 0.4 substitutions/site to minimize substitution saturation effects.

Following these criteria, we selected 215 sister lineages for mitochondrial genes and 165 sister lineages for nuclear genes (Datasets S17 and S26). Each sister pair consists of two families that share a common ancestor, with equal time for accumulating substitutions and diversification. Therefore, disparities in branch length and clade size reflect variations in molecular rates and net diversification, respectively. Differences in molecular rates were averaged across all possible species pairs within each sister pair, whereas clade sizes were derived from comprehensive taxonomic lists of extant species. Associations between the molecular rate and clade size differences were analyzed using ordinary least squares regression through the origin.

Data, Materials, and Software Availability. Script, all data, and SI datasets have been deposited in GitHub (https://github.com/tianlongcai/vertmolrate) (62). All other data are included in the manuscript and/or supporting information.

ACKNOWLEDGMENTS. We thank Jiansi Gao, Yalin Cheng, Wenwen Chen, Kangli Zhu, and Yan Hou for their suggestions on the data collection and analyses. We are grateful to Jianzhi Zhang and Kirk Lohmueller for their insightful comments on our earlier version of the manuscript. We thank the editor and two anonymous reviewers for their valuable comments. Special thanks to Shimiao Shao for assistance with language editing. We thank the Westlake Supercomputer Center for high-performance computing support. This work was supported by National Natural Science Foundation of China grants [32370662 (Y.Z.), 32100350 (T.C.)], the "Pioneer" and "Leading Goose" Zhejiang Province Key Research and Development Plan [2024SSYS0032], and the Research Center for Industries of the Future at Westlake University.

Author affiliations: [a]Westlake Laboratory of Life Sciences and Biomedicine, Hangzhou, Zhejiang 310024, China; [b]Research Center for Industries of the Future and School of Life Sciences, Westlake University, Hangzhou, Zhejiang 310030, China; [c]Institute of Biology, Westlake Institute for Advanced Study, Hangzhou, Zhejiang 310024, China; [d]State Key Laboratory of Animal Biodiversity Conservation and Integrated Pest Management, Institute of Zoology, Chinese Academy of Sciences, Beijing 100101, China; and [e]School of Resources and Environmental Engineering, Anhui University, Hefei 230601, China

1. H. Hillebrand, On the generality of the latitudinal diversity gradient. *Am. Ant.* **163**, 192–211 (2004).
2. G. G. Mittelbach *et al.*, Evolution and the latitudinal diversity gradient: Speciation, extinction and biogeography. *Ecol. Lett.* **10**, 315–331 (2007).
3. D. Jablonski, K. Roy, J. W. Valentine, Out of the tropics: Evolutionary dynamics of the latitudinal diversity gradient. *Science* **314**, 102–106 (2006).
4. J. F. Gillooly, A. P. Allen, Linking global patterns in biodiversity to evolutionary dynamics using metabolic theory. *Ecology* **88**, 1890–1894 (2007).
5. A. P. Allen, J. F. Gillooly, V. M. Savage, J. H. Brown, Kinetic effects of temperature on rates of genetic divergence and speciation. *Proc. Natl. Acad. Sci. U.S.A.* **103**, 9130–9135 (2006).
6. J. F. Gillooly, A. P. Allen, G. B. West, J. H. Brown, The rate of DNA evolution: Effects of body size and temperature on the molecular clock. *Proc. Natl. Acad. Sci. U.S.A.* **102**, 140–145 (2005).
7. D. Schluter, Evidence for ecological speciation and its alternative. *Science* **323**, 737–741 (2009).
8. O. Seehausen *et al.*, Genomics and the origin of species. *Nat. Rev. Genet.* **15**, 176–192 (2014).
9. K. Rohde, Latitudinal gradients in species diversity: The search for the primary cause. *Oikos* **65**, 514–527 (1992).
10. Á. Dugo-Cota, S. Castroviejo-Fisher, C. Vilà, A. Gonzalez-Voyer, A test of the integrated evolutionary speed hypothesis in a Neotropical amphibian radiation. *Global Ecol. Biogeogr.* **24**, 804–813 (2015).
11. L. N. Gillman, S. D. Wright, Species richness and evolutionary speed: The influence of temperature, water and area. *J. Biogeogr.* **41**, 39–51 (2014).
12. J. F. Gillooly, J. H. Brown, G. B. West, V. M. Savage, E. L. Charnov, Effects of size and temperature on metabolic rate. *Science* **293**, 2248–2251 (2001).
13. A. P. Martin, S. R. Palumbi, Body size, metabolic rate, generation time, and the molecular clock. *Proc. Natl. Acad. Sci. U.S.A.* **90**, 4087–4091 (1993).
14. A. E. McKechnie, Phenotypic flexibility in basal metabolic rate and the changing view of avian physiological diversity: A review. *J. Comp. Physiol. B* **178**, 235–247 (2008).
15. E. J. Glanville, S. A. Murray, F. Seebacher, Thermal adaptation in endotherms: Climate and phylogeny interact to determine population-level responses in a wild rat. *Funct. Ecol.* **26**, 390–398 (2012).
16. J. Avaria-Llautureo, C. E. Hernández, E. Rodríguez-Serrano, C. Venditti, The decoupled nature of basal metabolic rate and body temperature in endotherm evolution. *Nature* **572**, 651–654 (2019).
17. E. Dowle, M. Morgan-Richards, S. Trewick, Molecular evolution and the latitudinal biodiversity gradient. *Heredity* **110**, 501–510 (2013).
18. H. Liu, M. Sun, J. Zhang, Genomic estimates of mutation and substitution rates contradict the evolutionary speed hypothesis of the latitudinal diversity gradient. *Proc. R. Soc. B* **290**, 20231787 (2023).
19. B. Nabholz, R. Lanfear, J. Fuchs, Body mass-corrected molecular rate for bird mitochondrial DNA. *Mol. Ecol.* **25**, 4438–4449 (2016).
20. B. Nabholz, S. Glémin, N. Galtier, Strong variations of mitochondrial mutation rate across mammals–The longevity hypothesis. *Mol. Biol. Evol.* **25**, 120–130 (2008).
21. T. Ohta, The nearly neutral theory of molecular evolution. *Annu. Rev. Ecol. Syst.* **23**, 263–286 (1992).
22. M. Kimura, *The Neutral Theory of Molecular Evolution* (Cambridge University Press, New York, 1983).
23. A. P. Martin, G. J. Naylor, S. R. Palumbi, Rates of mitochondrial DNA evolution in sharks are slow compared with mammals. *Nature* **357**, 153–155 (1992).
24. D. L. Rabosky *et al.*, An inverse latitudinal gradient in speciation rate for marine fishes. *Nature* **559**, 392–395 (2018).
25. R. Allio, S. Donega, N. Galtier, B. Nabholz, Large variation in the ratio of mitochondrial to nuclear mutation rate across animals: Implications for genetic diversity and the use of mitochondrial DNA as a molecular marker. *Mol. Biol. Evol.* **34**, 2762–2772 (2017).
26. I. M. Sokolova, Ectotherm mitochondrial economy and responses to global warming. *Acta Physiol.* **237**, e13950 (2023).
27. J. Ivan *et al.*, Temperature predicts the rate of molecular evolution in Australian Eugongylinae skinks. *Evolution* **76**, 252–261 (2022).
28. X.-L. Chu *et al.*, Temperature responses of mutation rate and mutational spectrum in an *Escherichia coli* strain and the correlation with metabolic rate. *BMC Evol. Biol.* **18**, 1–8 (2018).
29. W. Jetz, R. P. Freckleton, A. E. McKechnie, Environment, migratory tendency, phylogeny and basal metabolic rate in birds. *PLoS One* **3**, e3261 (2008).
30. T. S. Fristoe *et al.*, Metabolic heat production and thermal conductance are mass-independent adaptations to thermal environment in birds and mammals. *Proc. Natl. Acad. Sci. U.S.A.* **112**, 15934–15939 (2015).
31. I. Khaliq, C. Hof, R. Prinzinger, K. Böhning-Gaese, M. Pfenninger, Global variation in thermal tolerances and vulnerability of endotherms to climate change. *Proc. Biol. Sci.* **281**, 20141097 (2014).
32. C. F. Mugal, J. B. Wolf, I. Kaj, Why time matters: Codon evolution and the temporal dynamics of d N/d S. *Mol. Biol. Evol.* **31**, 212–231 (2014).
33. B. Charlesworth, Effective population size and patterns of molecular evolution and variation. *Nat. Rev. Genet.* **10**, 195–205 (2009).
34. M. Lynch, Evolution of the mutation rate. *TRENDS Genet.* **26**, 345–352 (2010).
35. M. Lynch *et al.*, Genetic drift, selection and the evolution of the mutation rate. *Nat. Rev. Genet.* **17**, 704–714 (2016).
36. J. Avise, *Phylogeography: The History and Formation of Species* (Harvard University Press, London, 2000).
37. S. H. Eo, J. A. DeWoody, Evolutionary rates of mitochondrial genomes correspond to diversification rates and to contemporary species richness in birds and reptiles. *Proc. R. Soc. B: Biol. Sci.* **277**, 3587–3592 (2010).
38. A. M. Ritchie, X. Hua, L. Bromham, Diversification rate is associated with rate of molecular evolution in ray-finned fish (actinopterygii). *J. Mol. Evol.* **90**, 200–214 (2022).
39. R. Lanfear, S. Y. Ho, D. Love, L. Bromham, Mutation rate is linked to diversification in birds. *Proc. Natl. Acad. Sci. U.S.A.* **107**, 20423–20428 (2010).
40. D. Schluter, Speciation, ecological opportunity, and latitude. *Am. Ant.* **187**, 1–18 (2016).
41. M. G. Harvey, S. Singhal, D. L. Rabosky, Beyond reproductive isolation: Demographic controls on the speciation process. *Annu. Rev. Ecol. Evol. Syst.* **50**, 75–95 (2019).
42. A. Stamatakis, RAxML version 8: A tool for phylogenetic analysis and post-analysis of large phylogenies. *Bioinformatics* **30**, 1312–1313 (2014).
43. R. O. Prum *et al.*, A comprehensive phylogeny of birds (Aves) using targeted next-generation DNA sequencing. *Nature* **526**, 569–573 (2015).
44. C. H. Oliveros *et al.*, Earth history and the passerine superradiation. *Proc. Natl. Acad. Sci. U.S.A.* **116**, 7916–7925 (2019).
45. N. S. Upham, J. A. Esselstyn, W. Jetz, Inferring the mammal tree: Species-level sets of phylogenies for questions in ecology, evolution, and conservation. *PLoS Biol.* **17**, e3000494 (2019).
46. W. Jetz, R. A. Pyron, The interplay of past diversification and evolutionary isolation with present imperilment across the amphibian tree of life. *Nat. Ecol. Evol.* **2**, 850–858 (2018).
47. R. A. Pyron, Novel approaches for phylogenetic inference from morphological data and total-evidence dating in squamate reptiles (lizards, snakes, and amphisbaenians). *Syst. Biol.* **66**, 38–56 (2017).
48. T. J. Colston, P. Kulkarni, W. Jetz, R. A. Pyron, Phylogenetic and spatial distribution of evolutionary diversification, isolation, and threat in turtles and crocodilians (non-avian archosauromorphs). *BMC Evol. Biol.* **20**, 1–16 (2020).
49. S. A. Smith, B. C. O'Meara, treePL: Divergence time estimation using penalized likelihood for large phylogenies. *Bioinformatics* **28**, 2689–2690 (2012).
50. J. J. Welch, D. Waxman, Calculating independent contrasts for the comparative study of substitution rates. *J. Theor. Biol.* **251**, 667–678 (2008).
51. J. Sullivan, P. Joyce, Model selection in phylogenetics. *Annu. Rev. Ecol. Evol. Syst.* **36**, 445–466 (2005).
52. Z. Yang, PAML 4: Phylogenetic analysis by maximum likelihood. *Mol. Biol. Evol.* **24**, 1586–1591 (2007).
53. L. J. Revell, phytools: An R package for phylogenetic comparative biology (and other things). *Methods Ecol. Evol.* **3**, 217–223 (2012).
54. J. D. Hadfield, MCMC methods for multi-response generalized linear mixed models: The MCMCglmm R package. *J. Stat. Softw.* **33**, 1–22 (2010).
55. R. Bivand, G. Millo, G. Piras, A review of software for spatial econometrics in R. *Mathematics* **9**, 1276 (2021).
56. S. Nakagawa, H. Schielzeth, A general and simple method for obtaining R2 from generalized linear mixed-effects models. *Methods Ecol. Evol.* **4**, 133–142 (2013).
57. R. Lanfear, J. J. Welch, L. Bromham, Watching the clock: Studying variation in rates of molecular evolution between species. *Trends Ecol. Evol.* **25**, 495–503 (2010).
58. J. Stiller *et al.*, Complexity of avian evolution revealed by family-level genomes. *Nature* **629**, 851–860 (2024).
59. S. Álvarez-Carretero *et al.*, A species-level timeline of mammal evolution integrating phylogenomic data. *Nature* **602**, 263–267 (2022).
60. P. M. Hime *et al.*, Phylogenomics reveals ancient gene tree discordance in the amphibian tree of life. *Syst. Biol.* **70**, 49–66 (2021).
61. P. O. Title *et al.*, The macroevolutionary singularity of snakes. *Science* **383**, 918–923 (2024).
62. T. Cai, Z. Wen, Z. Jiang, Y. Zhen, VertMolRate: Datasets and scripts for analyzing latitudinal gradient in molecular rates and testing evolutionary speed hypothesis. GitHub. https://github.com/tianlongcai/vertmolrate. Deposited 26 April 2025.